Precision Agric (2010) 11:413–431
DOI 10.1007/s11119-010-9180-7

Spectral signatures of sugar beet leaves for the detection and differentiation of diseases

A.-K. Mahlein · U. Steiner · H.-W. Dehne · E.-C. Oerke

Published online: 13 June 2010

Abstract This study examines the potential of hyperspectral sensor systems for the non-destructive detection and differentiation of plant diseases. In particular, a comparison of three fungal leaf diseases of sugar beet was conducted in order to facilitate a simplified and reproducible data analysis method for hyperspectral vegetation data. Reflectance spectra (400–1050 nm) of leaves infected with the fungal pathogens *Cercospora beticola*, *Erysiphe betae*, and *Uromyces betae* causing *Cercospora* leaf spot, powdery mildew and rust, respectively, were recorded repeatedly during pathogenesis with a spectro-radiometer and analyzed for disease-specific spectral signatures. Calculating the spectral difference and reflectance sensitivity for each wavelength emphasized regions of high interest in the visible and near infrared region of the spectral signatures. The best correlating spectral bands differed depending on the diseases. Spectral vegetation indices related to physiological parameters were calculated and correlated to the severity of diseases. The spectral vegetation indices Normalised Difference Vegetation Index (NDVI), Anthocyanin Reflectance Index (ARI) and modified Chlorophyll Absorption Integral (mCAI) differed in their ability to assess the different diseases at an early stage of disease development, or even before first symptoms became visible. Results suggested that a distinctive differentiation of the three sugar beet diseases using spectral vegetation indices is possible using two or more indices in combination.

Keywords *Cercospora beticola* · *Erysiphe betae* · *Uromyces betae* · Sugar beet · Hyperspectral · Remote sensing · Disease detection · Spectral signature · Vegetation indices

A.-K. Mahlein (✉) · U. Steiner · H.-W. Dehne · E.-C. Oerke
Institute of Crop Science and Resource Conservation (INRES)—Phytomedicine, University of Bonn, Nussallee 9, 53115 Bonn, Germany
e-mail: amahlein@uni-bonn.de

Introduction

Sugar beet diseases are serious threats in worldwide sugar beet production. *Cercospora beticola* (Sacc.), *Erysiphe betae* (Vanha) Weltzien and *Uromyces betae* (Persoon) Lev., causing *Cercospora* leaf spot (CLS), powdery mildew (PM) and sugar beet rust (SBR), respectively, are the most relevant fungal leaf pathogens causing losses in yield quantity and quality. The three foliar diseases are associated with typical symptoms. The pertho-trophic pathogen *C. beticola* causes leaf spots with a reddish brown margin of typically 2–5 mm diameter. Under high temperature conditions and high relative humidity, the leaf spots coalesce to form large necrotic areas. The biotroph pathogen *E. betae* relies on the metabolism of sugar beet tissue as a nutrient source. Characteristic symptoms of PM are white, fluffy mycelia, which cover the upper and lower side of the leaf. Typical symptoms of SBR are small (0.5–1.5 mm) pustules, often encircled by a chlorotic ring, irregularly distributed over the leaves. Reddish-brown uredospores of the biotroph pathogen are released after rupturing the epidermal layer.

Leaf diseases of sugar beet are commonly controlled by planting resistant cultivars or by multiple fungicide applications. Due to high control costs and the environmental impact of fungicides, a site-specific application according to precision farming techniques i.e. monitor and manage spatially-variable fields site-specifically (Stafford 2000)—is of high interest. Therefore, a precise, reproducible and time-saving disease monitoring method is essential (Hillnhuetter and Mahlein 2008; Steddom et al. 2005). Nutter et al. (1990) pointed out that remote sensing techniques may provide an alternative to visually-based disease assessment. Technological advances in sensor development, in particular progress from multi-spectral broadband sensors to hyper-spectral narrowband sensors, have increased the quantity and quality of available information.

Spectral reflectance measurements are used for non-destructive assessment of the physiological status of vegetation (e.g. pigment content, leaf area), and to discriminate crop species or to detect the impact of stress such as plant diseases, drought stress or nutrition deficiencies (Blackburn 2007; Moran et al. 1997; Richardson et al. 2001). Leaf reflectance of sunlight in the visible (VIS, 400–700 nm) and near infrared (NIR, 700–1000 nm) are driven by multiple interactions: the scattering of light as a result of leaf surface and internal cellular structures, and radiant energy absorption induced by leaf chemistry. The function described by the ratio of the intensity of reflected light to the illuminated light for each wavelength forms the leaf/canopy spectral signature (Carter and Knapp 2001; Jones et al. 2003; West et al. 2003). Consequently, biophysical and biochemical attributes of vegetation can be derived by reflectance spectra. Optical methods such as hyper-spectral imaging and non-imaging sensors have been proved to be a useful tool to detect changes in plant vitality (Hatfield et al. 2008; Nilsson 1995; West et al. 2003). The best results for identifying diseases were obtained in the visible and near-infrared range of the spectrum.

Disease symptoms often result from physiological changes in plant metabolism brought about by the pathogen. The impact of plant diseases on the physiology and phenology of plants, however, varies with the host-pathogen interaction and may cause modifications in pigments (Gamon and Surfus 1999; Pinter et al. 2003), water content, functionality of tissue or the appearance of pathogen-specific structures. In fact, these individual impacts may alter the spectral pattern of the plant. Knowledge of the physiological effect of diseases on the metabolism and structures of plants are beneficial for hyper-spectral discrimination of healthy and diseased leaf and canopy elements (Moran et al. 1997).

Several studies have shown that remote sensing has a high potential for discriminating between healthy and stressed plants. Steddom et al. (2005) demonstrated that multispectral disease evaluation can be used to measure necrosis caused by CLS in sugar beets. The detection of rhizomania in sugar beet fields was also feasible (Steddom et al. 2003). Using a quadratic discriminating model based on reflectance, Bravo et al. (2003) classified yellow rust infestation on winter wheat with a reliability of 96%. Larsolle and Hamid Muhammed (2007) computed disease specific spectral signatures of *Drechslera tritici-repentis* infected spring wheat. Other researchers successfully used spectral data to detect *Phytophthora infestans* on tomato (Zhang et al. 2002) or *Venturia inaequalis* on apple trees (Delalieux et al. 2007). However, these studies are focused on the binary discrimination between highly diseased plants and healthy plants. More research is required about the specific effects of different diseases, the effect of disease stage and the impact of disease severity on spectral characteristics of plant species. These factors have to be taken into account for an assessment of sensor sensitivity.

It is necessary to implement appropriate techniques to characterize the main source of spectral variability and to identify optimal wavebands that offer maximum information content from reflectance data. Spectral vegetation indices (SVIs) are widely used for monitoring, analyzing and mapping temporal and spatial variation in vegetation (Gitelson et al. 2002). By calculating ratios of several bands at different ranges of the spectrum, SVIs result in a reduction of data dimension, which may be useful in effective data analysis for disease discrimination. SVIs are the basis for many applications of remote sensing in crop management because they are highly correlated to plant health or vitality. As pigment content provides information on the physiological state of leaves, pigment-specific SVIs may be also useful in detecting stresses caused by fungal diseases.

A fundamental challenge in using remote sensing techniques for stress detection is still the differentiation between different sources of stress. Most stress factors such as diseases, nutrient deficiency or water stress induce symptoms with little distinguishing spectral characteristics (Stafford 2000). However, an understanding of physiological responses of sugar beet plants to foliar diseases provides a more thorough interpretation of resultant impact on spectral signatures. For the purpose of this study, the relationships between different diseases and reflectance properties of sugar beet plants have been observed in detail at the leaf level. A multi-temporal approach was chosen to investigate the question whether it is possible to detect changes in the reflectance spectrum of infested sugar beet leaves before first symptoms became visible. Moreover, the potential of vegetation indices for early detection and discrimination of diseases was analysed.

Materials and methods

Plant cultivation

Sugar beet plants, cultivar Pauletta (KWS GmbH, Einbeck, Germany), were grown in a commercial substrate (Klasmann-Deilmann GmbH, Germany) in plastic pots (Ø 13 cm) in a controlled environment at 23/20°C (day/night), 60% relative humidity (RH) and a photoperiod of 16 h per day. Plants were watered as necessary and fertilized weekly with 100 ml of a 0.2% solution of Poly Crescal (Aglukon GmbH, Düsseldorf, Germany). For each treatment, 15 plants were inoculated with the different pathogens when four leaves were fully developed (Growth Stage 14, BBCH scale) (Meier et al. 1993).

Pathogens

Inoculum of *Cercospora beticola* was produced from wetted infected sugar beet leaves incubated for 24 h under 100% RH. A spore suspension with 40 000 spores per ml was sprayed onto the leaves of 15 healthy plants. After inoculation, the plants were covered with plastic bags to create 100% RH at 25/20°C for 48 h. For further incubation, the plants were transferred to 23/20°C and 60 ± 10% RH. Suspensions of *Uromyces betae* urediniospores, 40 000 spores per ml, harvested from sporulating uredia and stored at 8°C were sprayed onto 15 sugar beet leaves. The plants were covered with plastic bags for 48 h (100% RH) and were incubated in a climate chamber at 19/16°C. Then, the plants were transferred to 23/20°C and 60 ± 10% RH. Plants heavily infested with powdery mildew were used as an inoculum source of *Erysiphe betae*. Healthy plants were inoculated in a chamber where a ventilator ran for 5 s in order to distribute *E. betae* conidia evenly on the leaf surfaces. Plants were left overnight and subsequently transferred to a glasshouse at 23/20°C, separated from the other plants. A control group of 15 plants was kept non-inoculated at 23/20°C and 60 ± 10% RH.

Measurement of leaf reflectance

Spectral reflectance was measured with a handheld non-imaging spectro-radiometer using a plant probe foreoptic with a leaf clip holder (ASD FieldSpec Pro FR spectrometer, Analytic Spectral Devices, Boulder, USA). The spectral range was from 350 to 1100 nm. Because the reflectance spectra data were noisy at the extremes, values between 400 and 1050 nm were analyzed. The spectral sampling interval was automatically interpolated from 1.4 to 1 nm steps using a linear equation by the ASD software. The contact probe foreoptic has a 10 mm field of view and an integrated 100 W halogen reflector lamp. The instrument was warmed up for 90 min previous to measurement to increase the quality and homogeneity of spectral data. Instrument optimization and reflectance calibration were performed prior to sample acquisition. The average of 25 dark-current measurements was calibrated to the average of 25 barium sulphate white reference (Spectralon, Labsphere, North Sutton, NH, USA) measurements. Because of the internal light source, the integration time was adjusted to 17 ms per scan constantly. Finally, reflectance spectra were obtained by determining the ratio of recorded sample data to data acquired for the white reflectance standard. Each sample scan represented an average of 25 reflectance spectra.

Data of infected and non-infected leaves were collected and recorded daily up until 21 days after inoculation (dai). In each treatment, spectra from 15 plants and 2 leaves per plant from the adaxial leaf surface were taken. The two youngest, fully developed leaves of each plant were marked. Furthermore, digital RGB images of the leaves were taken. Disease severity of each pathogen was evaluated daily and classified according to Wolf and Verreet (2002).

Data analysis

Because reflectance spectra were assessed under constant light and temperature conditions with the plant probe foreoptic, pre-processing to smooth the spectrum and reduce signal noise was not necessary. In order to investigate in which wavelength significant differences occur between classes of disease severity, difference spectra were calculated by subtracting the mean reflectance of diseased sugar beets from mean reflectance of healthy sugar beets at each wavelength. Additionally, reflectance sensitivity for each wavelength was

Table 1 Vegetation indices and algorithms used in this study

Index	Equation[a]	Related to	Reference
Normalized difference vegetation index	NDVI = (R800 − R670)/(R800 + R670)	Biomass/leaf area	Rouse et al. (1974)
Structural independent pigment index	SIPI = (R800 − R445)/(R800 + R680)	Carotenoids: chlorophyll *a* ratio	Penuelas et al. (1995)
Pigments specific simple ratio	PSSRa = R800/R680 PSSRb = R800/R635	Chlorophyll (*a*/*b*)	Blackburn (1998)
Anthocyanin reflectance index	ARI = (1/R550) − (1/R700)	Anthocyanin	Gitelson et al. (2001)
Red edge position	R_{RE} = R670 + R780/2 REP = 700 + 40x (R_{RE} − R700)/(R740 − R700)	Inflection point red edge	Guyot and Baret (1988)
Modified chlorophyll absorption integral	mCAI = (R545 + R752)/2 * (752 − 545) − (∑R752:R545) (R * 1423)	Chlorophyll	Laudien (2005)

[a] Reflectance at wavelengths indicated

calculated as the reflectance of diseased leaves divided by the mean reflectance of healthy leaves. Changes in the spectral signature for each disease were evaluated by simple linear correlation analyses. With correlation curves, the intensity of the relationship of each narrow band of the spectrum was visualized and specific wavebands of the spectral signature closely related to disease infestation were selected.

To evaluate the efficiency of spectral vegetation indices (SVIs) to identify and discriminate between the different foliar diseases, SVIs related to different physiological parameters were calculated (Table 1). In this study, the normalized difference vegetation index (NDVI), the structural independent pigment index (SIPI), the pigment specific simple ratio for chlorophyll *a* and *b* (PSSRa/PSSRb) and the anthocyanin reflectance index (ARI) were used. In addition, the red edge position (REP) and the modified chlorophyll absorption integral (mCAI) were calculated. Correlation and regression analyses between vegetation indices and disease severities for each disease were conducted.

Statistical analyses

Statistically significant differences between treatments were calculated using the Superior Performing Software System SPSS 17.0 (SPSS Inc., Chicago, IL, USA). Data were analysed by standard analysis of variance (ANOVA). For significant *F*-values, homogeneous subgroups were built using the Tukey-test, with a significance level of $p = 0.05$. Relationships were determined by Pearson coefficient of correlation (r). The experiments were repeated twice.

Results

Reflectance spectra of diseased sugar beet plants

Reflectance measurements of non-inoculated leaves and leaves inoculated with the foliar diseases were conducted on 21 consecutive days following inoculation. During this period, reflectance curves of non-inoculated sugar beets were characteristic for healthy leaves and

remained largely constant with a strong absorption by photosynthetic pigments in the VIS and a high reflectance plateau in the NIR caused by multiple scattering, related to the internal structure of the leaf. Figure 1a–c summarize averaged spectral signatures of sugar beet leaves with *Cercospora* leaf spot, powdery mildew and sugar beet rust at 0, 10, 20, 50 and 80% disease severity, respectively. Compared to the spectral signature of healthy leaves, each disease had a characteristic, divergent reflectance curve. The changes in reflectance were strongly correlated to the occurrence of disease-specific symptoms. The development of diseases and the symptoms varied for the three pathogens (Table 2). Small chloroses were the first symptoms of CLS. After 6–8 days of incubation, the spots became necrotic and the characteristic red margin of the spots became visible. First symptoms of powdery mildew appeared 5 dai. Disease severity of powdery mildew increased rapidly. In the beginning, small colonies were visible on the upper side of leaves, and covered the total leaf surface 14 dai. First chloroses, due to *Uromyces betae*, became visible 9 dai. At later stages, rust spores ruptured the epidermis and amber uredinia became visible on the upper and lower sides of leaves.

Reflectance of *C. beticola*-infected leaves (Fig. 1a) increased in the VIS mostly in the green and red ranges of the spectrum (500–700 nm) and decreased in the NIR. With disease severities of 20 or 50%, higher reflectance values in the VIS could be detected. This was most pronounced between 450–530 and 550–700 nm. In the NIR, decreasing reflectance between 700–900 nm and increasing reflectance between 900 and 1050 nm was noticed. At a disease severity of 80%, reflectance increased over the whole spectrum and a typical spectral vegetation signature was no longer detectable. Maximal differences between healthy and CSL diseased leaves were in the VIS at 510, 690 nm and in the NIR at 740 nm for all disease severity levels (Fig. 3a). The wavelengths of maximum reflectance sensitivity to CLS were predominantly in the VIS between 450–500 and 600–700 nm with maximal values at 480 and 665 nm (Fig. 2a). Sensitivities were low in the NIR, in contrast to reflectance differences.

Reflectance of leaves colonized by the ectoparasite *E. betae* rose as disease severity increased (Fig. 1b). This increment was most distinctive in the VIS and least pronounced in the NIR. Powdery mildew affected the overall level of reflectance rather than the profile of the spectral signature. Differences were on a constant level between 400 and 700 nm, with a small peak at 700 nm and minor distinctive values between 720 and 1050 nm (Fig. 3b). Maximal reflectance sensitivity was between 400–530 and 570–700 nm (Fig. 2b). Sensitivity had a local minimum from 530 to 570 nm.

Due to the small symptoms of the biotroph *U. betae* scattered on the leaf area, changes of reflectance spectra were small (Fig. 1c). At 10% disease severity, the differences from healthy leaves were not significant. Reflectance of leaves with 20% disease severity was higher than healthy leaves from 550 to 700 nm. Explicit changes were measured at a disease severity of 50%; i.e. high reflectance between 550 and 700 nm and low reflectance between 700 and 900 nm. Wavelengths of maximum differences occurred from 500 to 670 nm; a peak at 700 nm was also detectable (Fig. 3c). In the NIR, there were negative differences from 720 to 800 nm. Sensitivity curve analysis indicated that the wavelength most sensitive to changes caused by SBR were from 500 to 670 nm (Fig. 2c). Also reflectance next to 700 nm was sensitive to SBR infection.

Relationship between spectral signatures and disease severity

The linear correlation coefficient (r) for disease severity versus reflectance varied considerably with the wavebands. Large differences were detected between the diseases

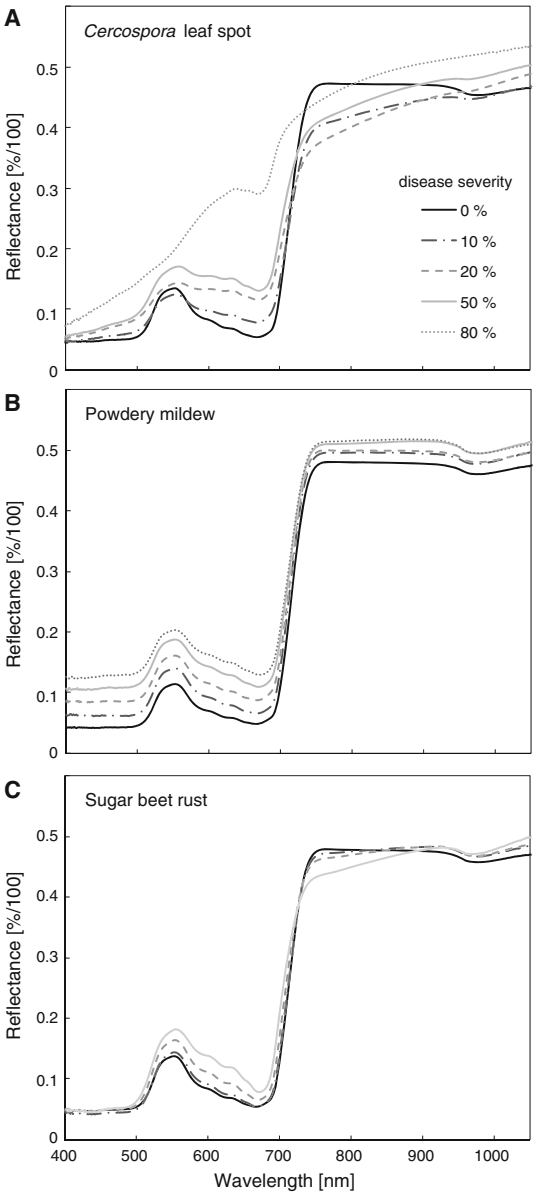

Fig. 1 **a–c**: Spectral signatures of sugar beet leaves affected with *Cercospora* leaf spot, powdery mildew and sugar beet rust at different disease severities. Reflectance was measured under controlled conditions

(Fig. 4). The correlation between CLS severity and reflectance was positive in the VIS range, with high values from 430 to 520 nm and from 570 to 710 nm (Fig. 4a). In the NIR, there was a negative correlation maximum around 740 nm. For PM severity, there was high correlation over the whole spectrum (Fig. 4b). In the VIS region, the correlation coefficients values were highest and reached $r = 0.85$. Displaying the correlation between SBR disease severity and reflectance, Fig. 4c indicates that wavelengths from 510 to 700 nm showed a strong positive correlation. In contrast to the other diseases, the

Table 2 Development of sugar beet leaf diseases expressed as percentage diseased leaf area according to Wolf and Verreet (2002)

Disease	Days after inoculation									
	1	2	3	4	5	6	7	8	9	10
Cercospora leaf spot	0	0	0	0	0	0.9	1.3	1.6	2	2.9
Powdery mildew	0	0	0	0	1.4	1.7	2.5	4.6	8.8	12
Sugar beet rust	0	0	0	0	0	0	0	0.6	0.9	1.1
Disease	Days after inoculation									
	11	12	13	14	15	16	17	18	19	20
Cercospora leaf spot	5.1	7.5	11	14.7	17.3	25.3	33.1	39.9	49.7	57.9
Powdery mildew	15.6	20.4	25.8	36.2	50.2	67	84.9	100	100	100
Sugar beet rust	1.5	2	2.9	4.9	9.7	13.8	17.6	23.3	34.1	42.5

correlation between SBR severity and wavelengths from 400 to 500 nm was weak. Similar to CLS, a negative correlation could be detected for SBR in the NIR. The different correlation coefficients between reflectance and a specific waveband for each disease indicated that reflectance at these wavelengths might be important for disease prediction.

Effect of disease progression on spectral vegetation indices

Seven SVIs related to different physiological plant parameters were calculated for each treatment and every day. Among the different diseases, the correlation between index values and disease severity varied (Table 3). Their suitability to distinguish between healthy and diseased sugar beets was proven. Regarding the biochemical modifications of the diseased plants, some indices were more suitable than others (Table 4). The NDVI was most sensitive to increase in disease severity of CLS and PM. Significant differences to healthy plants could be detected 8 dai for both diseases. The relation between NDVI and SBR was less pronounced. Changes between SBR infected and healthy plants could be measured 13 dai. The SIPI was best applicable for the detection of PM, significant differences could be detected 7 dai. There was also a strong correlation between SIPI and CLS; CLS infected plants could be separated from healthy plants as early as 8 dai. The correlation between SIPI and SBR was low, thus, discrimination from healthy plants was not significant before 17 dai. Similar results could be calculated for PSSRa; high correlation to CLS and PM and lower correlation to SBR. Significant differences to healthy sugar beets were recorded for CLS, PM and SBR 7, 8, and 10 dai, respectively. The chlorophyll b specific index PSSRb had the highest correlation to PM, lower to CLS and lowest to SBR severity. The ARI and REP were highly sensitive in distinguishing diseased from healthy sugar beet leaves. Even though the relation to disease severity was less distinctive, both SVIs resulted in values significantly different from healthy plants for all three diseases as early as 7 dai. The mCAI fitted best for CLS and SBR and less for PM. Significant differences were noticed for CLS and SBR 7 dai, for PM 10 dai.

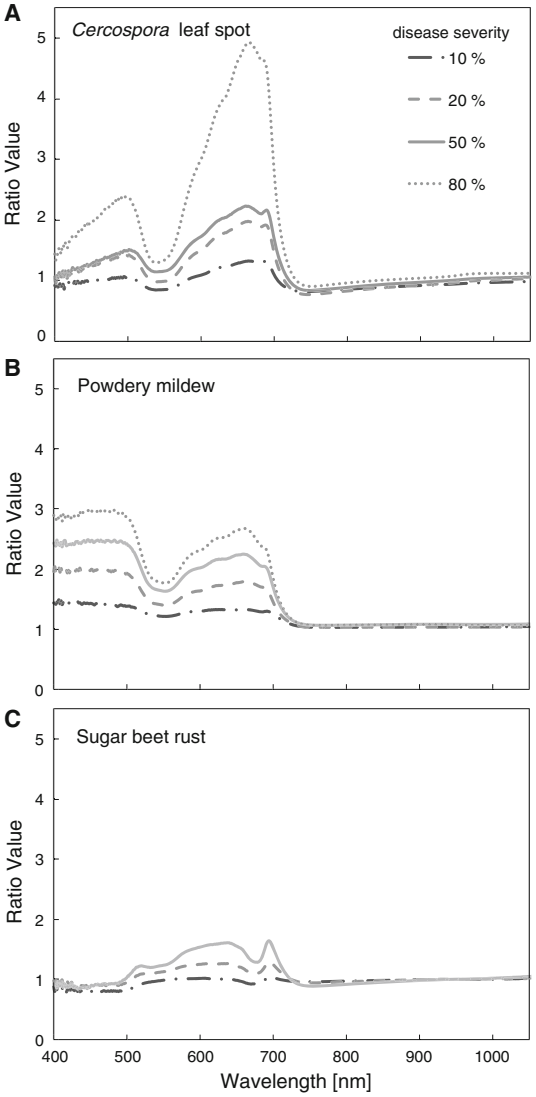

Fig. 2 **a–c**: Ratio values of sugar beet leaves affected with *Cercospora* leaf spot, powdery mildew and sugar beet rust at different disease severities. Non-dimensional ratio-values were computed by dividing reflectance of diseased leaves by reflectance of healthy leaves

Use of combinations of spectral vegetation indices for disease detection and identification

The results presented above allow only a classification between healthy and diseased plants. In a first approach, index combinations were tested to classify different disease treatments more specifically. Scatter matrices for all index combinations were mapped and the best differentiating combinations were examined (Fig. 5). Divergent scatter plots denoted robust index combinations to distinguish between the different diseases. Plots of SIPI, PSSRa, PSSRb and NDVI versus each other resulted in stacked scatter plots; the discriminative potential of these combinations was low. All combinations including the

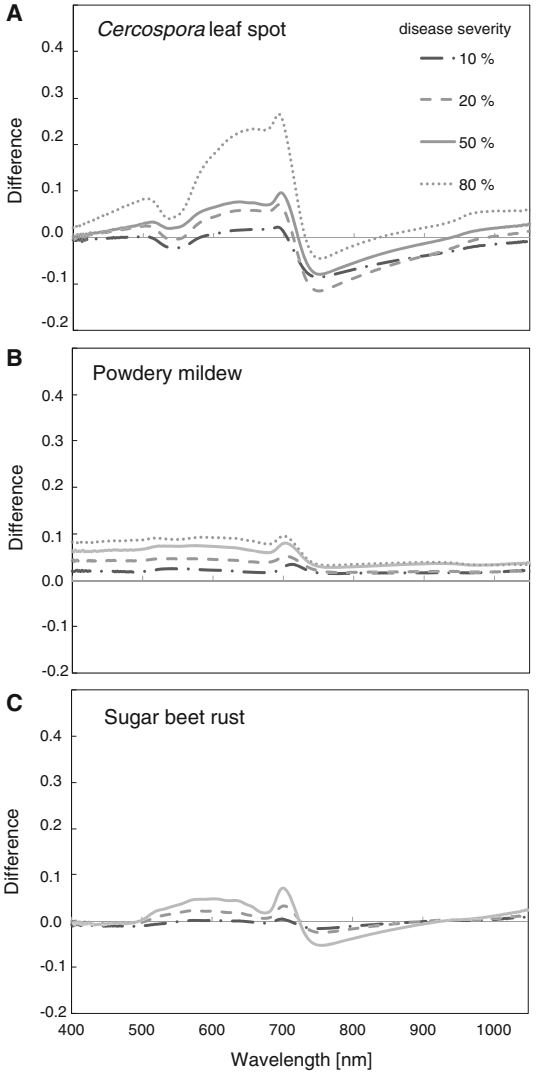

Fig. 3 **a–c**: Difference spectra of sugar beet leaves affected with *Cercospora* leaf spot, powdery mildew and sugar beet rust at different disease severities. Non-dimensional differences were computed by subtracting reflectance of healthy leaves from that of diseased leaves

ARI showed obvious divergent scatter plots for the diseases. Most distinctive differences were observed for the combination ARI versus SIPI and ARI versus NDVI. In particular, similar results could be noticed for mCAI versus ARI. The combination ARI versus SIPI showed that the severity of diseases biased the scatter plots (Fig. 6). Values from leaves with low disease severity were placed in the same region of the plot, irrespective of the disease. With increasing disease severity, CLS values changed to minor SIPI values and increasing ARI values. For higher SBR severities only, an increase in ARI values could be observed, whereas the SIPI remained constant. The distribution of PM values was highly divergent; with constant ARI values, SIPI values explicitly decreased with increasing disease severity.

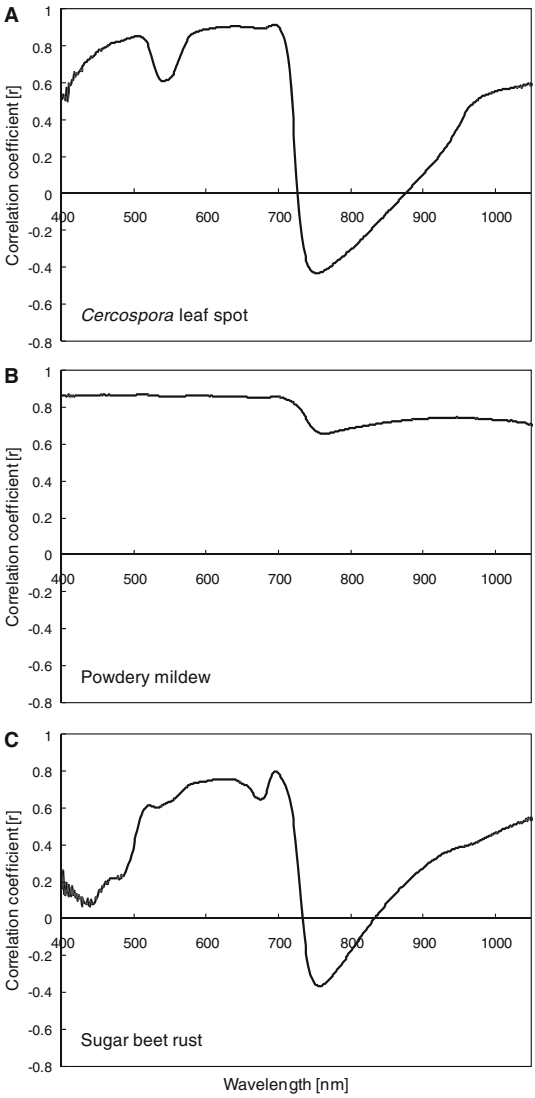

Fig. 4 Diagram of coefficient of correlation (r) for the linear correlation between spectral reflectance of sugar beet leaves and disease severity in relation to wavelength for **a** *Cercospora* leaf spot, **b** powdery mildew, and **c** sugar beet rust

Discussion

Identifying a specific disease or stress using remote sensing techniques still constitutes a significant challenge in vegetation monitoring. Qualitative and/or quantitative differences in the spectral reflectance between healthy and diseased plants have to be analyzed. Hence, an optical differentiation of healthy and diseased plants may be based on spectral measurements of different wavebands or on a combination of wavebands (West et al. 2003). Visible light is largely absorbed by pigments. The reflectance of wavelengths in the NIR range depends on the leaf structure, which causes multiple scattering within the leaf, related to the fraction of air spaces (Jacquemoud and Baret 1990). To classify various fungal diseases in the field using hyperspectral sensors, proper knowledge on the specific

Table 3 Coefficients of correlation between disease severity and seven spectral vegetation indices for three leaf diseases of sugar beet

Index	*Cercospora* leaf spot	Powdery mildew	Sugar beet rust
NDVI	−0.89	−0.89	−0.70
SIPI	−0.87	−0.89	−0.51
PSSRa	−0.84	−0.84	−0.64
PSSRb	−0.77	−0.84	−0.61
ARI	0.77	0.54	0.65
mCAI	−0.87	−0.77	−0.84
REP	0.75	0.58	0.62

spectral signatures caused by the developing diseases is essential. For that reason, a multitemporal approach under controlled conditions at the leaf level was chosen to collect and compare spectral signatures of foliar sugar beet diseases. In situ leaf reflectance measurements indicated specific spectral signatures for each disease.

Physiological interactions between a fungal disease and its host plant vary depending on the pathogen (Jones and Dangl 2006; van Kan 2006; Knogge 1996). The pattern of responses and the degree of up- and down-regulation of each physiological process are related to the type of host-pathogen relationship. Whereas perthotrophs (e.g. *Cercospora beticola*) rapidly kill plant cells to feed subsequently on the dead tissue, other fungi maintain biotroph relationships (powdery mildews: ectoparasite with haustoria within epidermal cells; rust fungi: endoparasite with intercellular growth and haustoria within parenchyma cells) with their host plants (Mendgen and Hahn 2002). Comparative observations of the three sugar beet pathogens suggested that the influence on the spectral signature depends on the intensity of physiological changes and on the extent of the symptoms. Malthus and Madeira (1993) pointed out that disease detection and assessment by means of reflectance spectra is feasible for diseases causing changes in pigments (VIS) or cell structure (NIR). Composition and content of leaf pigments change when the plant is exposed to phytopathogens that induce chlorotic- and necrotic-like symptoms (Carter and Knapp 2001; Jing et al. 2007; Pietrzykowski et al. 2006). Symptoms of the perthotrophic pathogen *C. beticola* are a consequence of the biological activity of cercosporin in the host cells (Daub and Ehrenshaft 2000). This fungal toxin leads to membrane damage and cell death after the fungus has penetrated the leaf through stomata to manipulate plant physiology to the benefit of the pathogen (Daub and Ehrenshaft 2000; Knogge 1996). Changes in spectral signature of CLS resulted from comparatively large necrotic areas. These localized, early infection stage non-uniform patches of necrotic tissue are immediately surrounded by healthy tissue. Due to senescent tissue and the accumulation of brown and reddish brown pigments, reflectance values of CLS spectra significantly increase between 600 and 700 nm.

At early disease stages, the impact of PM on the chlorophyll content is small, since the biotrophic fungus on the plant surface relies on the photosynthetic activity of the host tissue (Francis 2002). Hence, no peaks in the chlorophyll absorption bands of PM diseased leaves could be detected. Our results indicate that specific regions of the spectrum rather than one or two wavelengths have discriminating potential. A general decrease of reflection was detected because PM covers the leaf surface with the characteristic white mycelia. This effect, caused by the specific reflection of fungal tissue on the host plant, has not yet been described in the literature.

Table 4 Effect of disease progress of *Cercospora* leaf spot, powdery mildew, and sugar beet rust, respectively, on seven spectral vegetation indices of sugar beet leaves 1–20 days after inoculation

Index	Treatment	Days after inoculation												
		1[a]	5	6	7	8	9	10	11	12	14	16	18	20
NDVI	Healthy	0.78 a	0.80 a	0.80 b	0.81 a	0.81 ab	0.81 a	0.81 a	0.81 a	0.81 a	0.81 a	0.81 a	0.81 a	0.81 a
	CLS	0.81 a	0.80 a	0.80 b	0.80 a	0.79 c	0.78 b	0.75 b	0.74 b	0.72 b	0.68 c	0.63 c	0.58 c	0.52 b
	PM	0.81 a	0.81 a	0.81 ab	0.80 a	0.80 bc	0.78 b	0.76 b	0.74 b	0.70 c	0.66 c	0.62 c	0.60 c	0.49 d
	SBR	0.80 a	0.81 a	0.82 a	0.81 a	0.82 a	0.81 a	0.80 a	0.80 a	0.81 a	0.78 b	0.77 b	0.75 b	0.72 c
SIPI	Healthy	0.79 a	0.81 a	0.81 a	0.81 ab	0.81 ab	0.81 a	0.81 a	0.80 a	0.81 a	0.81 a	0.81 a	0.80 a	0.80 a
	CLS	0.81 a	0.80 a	0.81 a	0.81 ab	0.80 cb	0.79 b	0.77 b	0.76 b	0.75 b	0.72 b	0.70 b	0.67 c	0.63 c
	PM	0.82 a	0.81 a	0.81 a	0.80 b	0.80 c	0.78 c	0.76 b	0.74 c	0.70 c	0.66 c	0.62 c	0.61 d	0.51 d
	SBR	0.80 a	0.82 a	0.82 a	0.82 a	0.82 a	0.81 a	0.81 a	0.80 a	0.81 a	0.80 a	0.79 a	0.78 b	0.77 b
PSSRa	Healthy	7.70 a	8.43 a	8.62 b	8.99 a	8.85 ab	8.74 a	8.59 a	8.56 a	8.89 a	8.62 a	8.81 a	8.82 a	8.72 a
	CLS	8.64 a	8.27 a	8.62 b	8.39 b	8.12 c	7.68 b	6.76 b	6.54 b	5.95 b	5.12 c	4.49 c	3.77 c	3.22 c
	PM	9.00 a	8.77 a	9.15 a	8.50 ab	8.30 bc	7.59 b	6.97 b	6.51 b	5.40 c	4.72 c	4.27 c	3.95 c	3.01 c
	SBR	8.39 a	8.95 a	8.88 b	9.00 a	9.06 a	8.39 a	8.32 a	8.11 a	8.57 a	7.74 b	7.05 b	6.51 b	5.83 b
PSSRb	Healthy	6.68 a	7.77 a	7.94 a	8.25 a	8.46 a	8.37 a	8.21 a	8.22 a	8.46 a	8.34 a	8.53 a	8.23 a	8.22 a
	CLS	8.03 a	7.81 a	7.95 a	7.94 a	7.57 b	7.02 b	6.12 c	5.89 c	5.49 c	4.72 b	4.01 c	3.40 c	2.90 c
	PM	8.21 a	8.26 a	8.09 a	7.86 a	7.67 b	6.98 b	6.31 c	6.01 c	5.04 c	4.47 b	3.92 c	3.67 c	2.68 c
	SBR	7.88 a	8.42 a	8.39 a	8.07 a	8.36 a	7.91 a	7.42 b	7.38 b	7.73 b	6.56 c	6.07 b	5.38 b	4.92 b
ARI	Healthy	−0.80 a	−0.63 a	−0.71 a	−0.74 a	−0.72 a	−0.73 a	−0.66 a	−0.64 a	−0.67 a	−0.71 a	−0.74 a	−0.75 a	−0.73 a
	CLS	−0.19 a	−0.14 a	−0.18 b	−0.02 c	0.05 b	0.21 c	0.73 d	0.88 c	1.00 d	1.29 c	1.37 d	1.70 d	1.82 d
	PM	−0.65 a	−0.07 ab	−0.41 b	−0.18 b	−0.22 b	−0.32 b	0.10 c	0.05 b	0.16 c	0.04 b	0.10 b	0.20 b	0.28 b
	SBR	−0.05 a	−0.21 a	−0.22 b	−0.31 b	−0.32 c	−0.21 b	−0.15 b	−0.08 b	−0.17 b	−0.02 b	0.43 c	0.71 c	1.26 c

Table 4 continued

Index	Treatment	Days after inoculation												
		1[a]	5	6	7	8	9	10	11	12	14	16	18	20
mCAI	Healthy	31.87 a	31.71 a	31.76 a	31.60 a	31.84 b	32.44 a	31.99 a	31.72 a	31.48 a	30.91 a	31.92 a	31.02 a	32.26 a
	CLS	30.52 a	30.94 a	30.22 b	29.55 c	29.57 c	27.84 c	24.97 c	24.30 c	24.43 c	21.83 c	19.76 c	16.93 d	14.49 d
	PM	32.53 a	31.66 a	31.25 a	31.37 a	33.06 a	32.69 a	30.53 b	31.11 ab	29.46 b	30.47 a	28.08 b	28.04 b	22.43 c
	SBR	31.04 a	30.73 ab	30.51 b	30.69 b	31.21 b	31.16 b	29.86 b	30.33 b	31.19 a	29.42 b	28.67 b	26.46 c	24.22 b
REP	Healthy	717.1 a	718.2 a	718.6 a	718.9 a	718.6 a	718.7 a	718.7 a	718.8 a	719.2 a	719.0 a	718.9 a	719.0 a	718.8 a
	CLS	717.5 a	717.8 a	718.1 a	717.8 c	717.9 b	717.6 b	717.4 b	717.3 b	716.9 c	716.2 b	714.8 c	712.8 d	711.6 b
	PM	718.5 a	718.2 a	718.2 a	718.3 b	717.6 b	717.5 b	717.1 b	717.2 b	716.8 c	716.4 b	716.6 b	716.0 b	712.7 b
	SBR	717.0 a	717.4 a	717.6 b	717.6 c	717.4 b	717.2 b	717.2 b	717.2 b	717.4 b	716.5 b	715.3 c	714.2 c	713.1 b

NDVI normalized difference vegetation index, *SIPI* structure insensitive vegetation index, *PSSRa* pigments specific simple ratio chlorophyll *a*, *PSSRb* pigments specific simple ratio chlorophyll *b*, *ARI* anthocyanine reflectance index, *mCAI* modified chlorophyll absorption integral, *CLS Cercospora* leaf spot, *PM* powdery mildew, *SBR* sugar beet rust

For each index, means within a row followed by the same letters are not significantly different according to ANOVA and Tukey-test ($p > 0.05$)

[a] From day 1 to day 6 there were no significant differences between healthy and diseased treatments; highlighted date indicates first appearance of visible disease symptoms

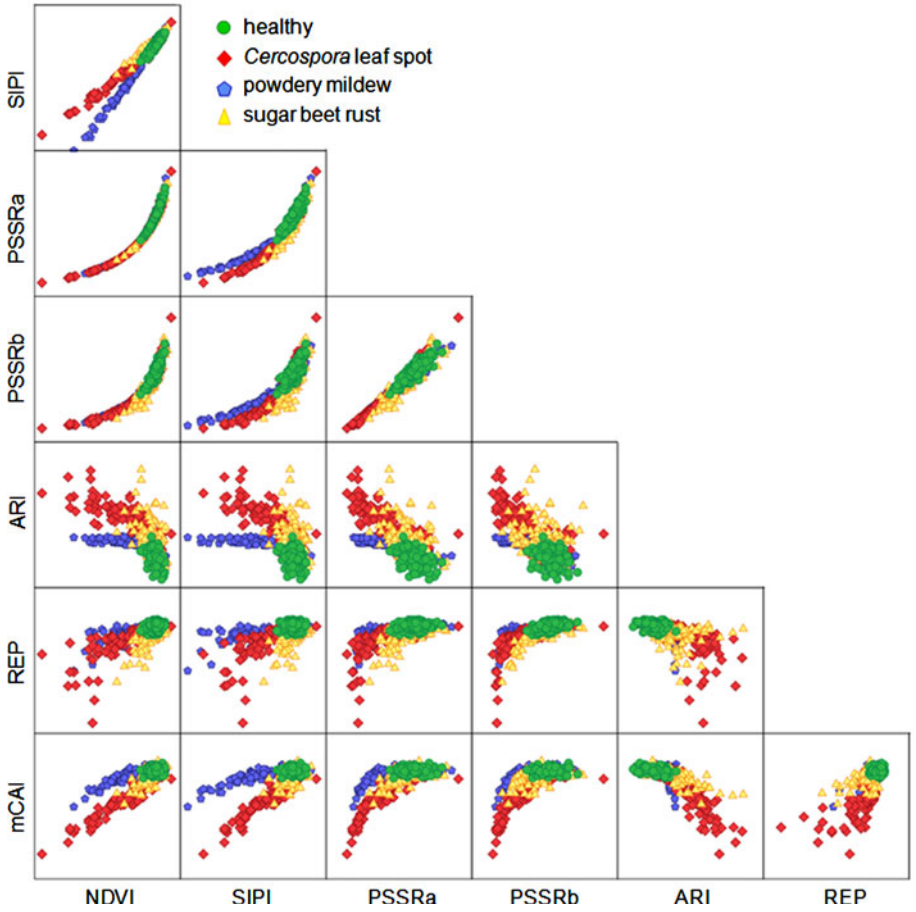

Fig. 5 Scatter matrix of different vegetation indices combinations for the discrimination of three leaf diseases of sugar beet, divergent scatter-plots denote a robust index combination for disease detection and discrimination. Best divergent combinations are ARI vs. NDVI, ARI vs. SIPI, mCAI vs. ARI and in particular mCAI vs. SIPI

Like *E. betae*, *U. betae* is a biothrophic pathogen, feeding from living plant cells and not apparently triggering any obvious adverse plant response (Heath 1997). Uredinia scattered on the leaf were small and numerous. The spectral differences caused by SBR were comparatively low, as the spectra acquired by a non-imaging spectro-radiometer are always a mixed signal of reflectance of tiny diseased areas and dominating healthy plant tissue.

According to Carter and Knapp (2001) who linked spectral characteristics to stress and chlorophyll concentration, the simple subtraction of healthy spectra and spectra representing the diseased leaves showed clearly the responses of the different spectral regions. The strongest linear relationship with total chlorophyll content is near 700 nm (Carter and Knapp 2001; Gitelson et al. 2003). Hence, the response of leaves diseased with CLS and SBR was more pronounced in this range than the response of PM. In contrast to the results of Steddom et al. (2005), who measured CLS of sugar beet with a multi-spectral radiometer

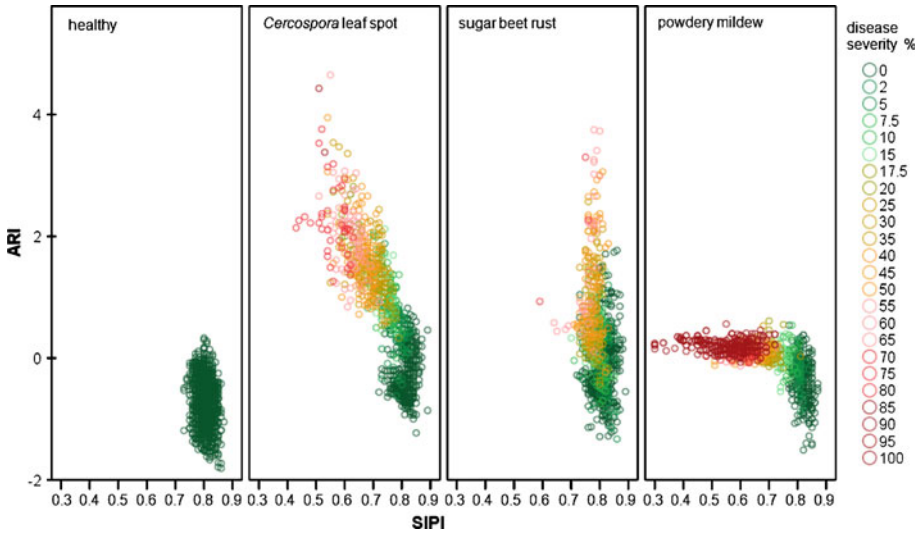

Fig. 6 Scatter matrix between the two spectral vegetation indices ARI and SIPI for each treatment of sugar beet leaves. Different colours display disease severity. Each treatment has a typical orientation in the co-ordinate system, thus a differentiation using this index combination seems feasible

in the field, we detected high correlations at wavelengths from 450 to 520 nm and from 570 to 710 nm. These deviations may be due to the use of a different sensor system used in our study (hyperspectral with 1 nm resolution versus multi-spectral with nine bands), and the differing measurement circumstances (field versus lab; constant light conditions versus sunlight). Jing et al. (2007) estimated a strong linear correlation between chlorophyll a concentration and yellow rust disease severity in wheat around 700 nm. In further data analyses, best correlating wavelength could be used for ratio development according to Richardson et al. (2001) and Carter and Knapp (2001).

Different changes in the spectral signatures not only denoted the occurrence of a disease but also provided information about the different developmental stages and severities of the disease. Delalieux et al. (2009) demonstrated that the discriminatory performances of spectral vegetation indices for apple scab due to *Venturia inaequalis* depended on the stage of infection and also on the phenological stage of apple leaves. Reflectance spectra of rice infected with rice panicle blast at different stages of grain development showed divergent characteristics over the developmental period (Kobayashi et al. 2001).

For early detection and for site-specific plant protection, SVIs have to be sensitive to changes in the reflection caused by diseases. Similarly, they have to be disease/stress specific. Several studies have estimated the potential of vegetation indices for early disease detection (e.g. Delalieux et al. 2009; Naidu et al. 2009; Steddom et al. 2005). Most developed indices are highly correlated with pigment content, biomass or leaf area (Le Maire et al. 2004; Thenkabail et al. 2000). Common indices from remote sensing, however, are neither disease- nor stress-specific. Nevertheless, SVIs showed promising results in studies assessing only one disease. A general classification into healthy and diseased plants using one SVI is possible. In these investigations, the three diseases affected the reflectance of sugar beet leaves in different ways. Comparing the correlation between SVIs and disease severity of each disease, significant differences according to the diseases could be detected.

These results lead to the conclusion that there is an increased potential of SVI-combinations for hyperspectral disease detection and discrimination. First analysis confirmed the idea that combinations of SVIs are useful for discriminating between healthy and diseased plants and even between the diseases in very early stages. Spectral vegetation indices based on different wavelengths describing different physiological parameters showed divergent scatter plots for healthy plants and illustrated each disease separately. Spectral vegetation indices based on similar wavelengths of the spectrum are highly correlated to each other, and hence not feasible for discrimination. Based on the knowledge compiled in this study, the sensor technology used may be applied also in the field (Mahlein et al. 2009). As Hatfield et al. (2008) mentioned out, the results from remote sensing methods in agriculture vary by the scale of observation, type of vegetation or variety and the sophistication of the model. Under these conditions, SVIs have the advantage that effects of different light intensities are reduced by calculating the ratio between different wavelengths instead of using absolute reflectance values. But there are still several difficulties and specifics in practice, like mixed infection with various pathogens, changing weather conditions and canopy structure. Disease-specific spectral signatures may be used as the basis for a spectral library of sugar beet diseases at different development stages for further classification methods.

The analysis of spectral information represents the basis for the development of disease indices depending on only a few wavelengths that can be assessed by a higher number of low-cost sensors. This is a precondition for high performance on large field areas and, therefore, for the introduction of disease sensing into agricultural practice driven by farmer's acceptance. This is true not only for arable crops, but also for fruits, vegetable crops and ornamentals.

Conclusions

The objective of this paper was the detection and differentiation of three fungal sugar beet leaf diseases using hyperspectral data. The experiments were conducted under laboratory condition to investigate the principles of the effect of diseases on reflectance of leaves. The spectral signatures of leaves under the effect of the three diseases were significantly different. The differences are based on the characteristic effect of each pathogen on biochemistry and physiology of sugar beet plants. The causal relationship between diseases and specific spectral changes is stressed by their dependence on the severity of diseases. Spectral vegetation indices are useful for the differentiation between healthy and diseased plants, and some are also useful for disease quantification. Our results, however, also suggest that single SVIs lack the potential to differentiate among diseases, not to mention the additional effects of abiotic plant stress, e.g. drought stress, nutrient deficiencies likely to occur in the field. The use of SVI combinations seems to be highly promising to improve disease detection and assignment versus biotic and abiotic plant stress.

Acknowledgments This study has been conducted within the Research Training Group 722 'Information Techniques for Precision Crop Protection', funded by the German Research Foundation (DFG). The authors further would like to thank Prof. Gunter Menz, Dr. Jonas Franke and Thorsten Mewes who provided the ASD FieldSpec Pro FR spectrometer and for technical assistance during hyperspectral measurements.

References

Blackburn, G. A. (1998). Quantifying chlorophylls and carotenoids at leaf and canopy scale: An evaluation of some hyperspectral approaches. *Remote Sensing of the Environment, 66*, 273–285.

Blackburn, G. A. (2007). Hyperspectral remote sensing of plant pigments. *Journal of Experimental Botany, 58*, 844–867.

Bravo, C., Moushou, D., West, J., McCartney, A., & Ramon, H. (2003). Early disease detection in wheat fields using spectral reflectance. *Biosystems Engineering, 84*, 137–145.

Carter, G. A., & Knapp, A. K. (2001). Leaf optical properties in higher plants: Linking spectral characteristics to stress and chlorophyll concentration. *American Journal of Botany, 88*, 677–684.

Daub, M. E., & Ehrenshaft, M. (2000). The photoactivated *Cercospora* toxin cercosporin: Contributions to plant disease and fundamental biology. *Annual Review of Phytopathology, 38*, 461–490.

Delalieux, S., Somers, B., Verstaeten, W. W., Van Aardt, J. A. N., Keulemans, W., & Coppin, P. (2009). Hyperspectral indices to diagnose leaf biotic stress of apple plants, considering leaf phenology. *International Journal of Remote Sensing, 30*, 1887–1912.

Delalieux, S., van Aardt, J., Kelemans, W., & Coppin, P. (2007). Detection of biotic stress (*Venturia inaequalis*) in apple trees using hyperspectral data: Non-parametric statistical approaches and physiological implications. *European Journal of Agronomy, 27*, 130–143.

Francis, S. (2002). Sugar-beet powdery mildew (*Erysiphe betae*). *Molecular Plant Pathology, 3*, 119–124.

Gamon, J. A., & Surfus, J. S. (1999). Assessing leaf pigment content and activity with a reflectometer. *New Phytologist, 143*, 105–117.

Gitelson, A. A., Gritz, Y., & Merzylak, M. N. (2003). Relationships between leaf chlorophyll content and spectral reflectance and algorithms for non-destructive chlorophyll assessment in higher plant leaves. *Journal of Plant Physiology, 160*, 271–282.

Gitelson, A. A., Kaufman, Y. J., Stark, R., & Rundquist, D. (2002). Novel algorithms for remote estimation of vegetation fraction. *Remote Sensing of the Environment, 80*, 76–87.

Gitelson, A. A., Merzlyak, M. N., & Chivkunova, O. B. (2001). Optical properties and nondestructive estimation of anthocyanin content in plant leaves. *Photochemistry and Photobiology, 74*, 38–45.

Guyot, G., & Baret, F. (1988). Utilisation de la haute résolution spectrale pour suivre l'état des couverts végétaux [Utilisation of high spectral resolution for monitoring vegetation condition]. In T. D. Guyenne & J. J. Hunt (Eds.), *Proceedings of 4th international colloquim spectral signatures of objects in remote sensing*, proceedings of the conference held 18–22 January 1988 in Aussois (Modane), France (pp. 279–286). ESA SP-287. European Space Agency

Hatfield, J. L., Gitelson, A. A., Schepers, J. S., & Walthall, C. L. (2008). Application of spectral remote sensing for agronomic decisions. *Agronomy Journal, 100*, 117–131.

Heath, M. C. (1997). Signalling between pathogenic rust fungi and resistant of susceptible host plants. *Annals of Botany, 80*, 713–720.

Hillnhuetter, C., & Mahlein, A.-K. (2008). Early detection and localisation of sugar beet diseases: New approaches. *Gesunde Pflanzen, 60*(4), 143–149.

Jacquemoud, S., & Baret, F. (1990). PROSPECT: A model of leaf optical properties spectra. *Remote Sensing of Environment, 34*, 75–91.

Jing, L., Jinbao, J., Yunhao, C., Yuanyuan, W., Wei, S., & Wenjiang, H. (2007). Using hyperspectral indices to estimate foliar chlorophyll a concentrations of winter wheat under yellow rust stress. *New Zealand Journal of Agricultural Research, 50*, 1031–1036.

Jones, H. G., Archer, N., Rotenburg, E., & Casa, R. (2003). Radiation measurement for plant ecophysiology. *Journal of Experimental Botany, 54*, 879–889.

Jones, J. D. G., & Dangl, J. L. (2006). The plant immune system. *Nature, 444*, 323–329.

Knogge, W. (1996). Fungal infections of plants. *The Plant Cell, 8*, 1711–1722.

Kobayashi, T., Kanda, E., Kitada, K., Ishiguro, K., & Torigoe, Y. (2001). Detection of rice panicle blast with multispectral radiometer and the potential of using airborne multispectral scanners. *Phytopathology, 91*, 316–323.

Larsolle, A., & Hamid Muhammed, H. (2007). Measuring crop status using multivariate analysis of hyperspectral field reflectance with application to disease severity and plant density. *Precision Agriculture, 8*, 37–47.

Laudien, R. (2005). Entwicklung eines GIS-gestützten schlagbezogenen Führungsinformationssystems für die Zuckerwirtschaft. [Development of a field- and GIS-based management information system for the sugar beet industry] PhD thesis, University of Hohenheim.

Le Maire, G., Francois, C., & Dufrene, E. (2004). Towards universal broad leaf chlorophyll indices using PROSPECT simulated database and hyperspectral reflectance measurements. *Remote Sensing of Environment, 89*, 1–28.

Mahlein, A.-K., Hillnhütter, C., Mewes, T., Scholz, C., Steiner, U., Dehne, H.-W., & Oerke, E.-C. (2009). Disease detection in sugar beet fields: A multi-temporal and multi-sensoral approach on different scales. In C. M. U. Neale & A. Maltese (Eds.), *Proceedings of the SPIE Europe conference on remote sensing* (Vol. 7472, pp. 747228–747228-10).

Malthus, T. J., & Madeira, A. C. (1993). High resolution spectroradiometry: Spectral reflectance of field bean leaves infected by *Botrytis fabae*. *Remote Sensing of Environment, 45*, 107–116.

Meier, U., Bachmann, L., Buhtz, H., Hack, H., Klose, R., Märländer, B., et al. (1993). Phänologische Entwick-lungsstadien der Beta-Rüben (*Beta vulgaris* L. ssp.). Codierung und Beschreibung nach der erweiterten BBCH-Skala (mit Abbildungen). [Phenological growth stages of sugar beet (*Beta vulgaris* L. ssp.) Codification and description according to the general BBCH scale (with figures).]. *Nachrichtenbl Deut Pflanzenschutzd, 45*, 37–41.

Mendgen, K., & Hahn, M. (2002). Plant infection and the establishment of fungal biotrophy. *Trends in Plant Science, 7*, 352–356.

Moran, M. S., Inoue, Y., & Barnes, E. M. (1997). Opportunities and limitations for image-based remote sensing in precision crop management. *Remote Sensing of the Environment, 61*, 319–346.

Naidu, R. A., Perry, E. M., Pierce, F. J., & Mekuria, T. (2009). The potential of spectral reflectance technique for the detection of grapevine leafroll-associated virus-3 in two red-berried wine grape cultivars. *Computers and Electronics in Agriculture, 66*, 38–45.

Nilsson, H.-E. (1995). Remote sensing and image analysis in plant pathology. *Annual Review of Phytopathology, 15*, 489–527.

Nutter, F. W., Jr., Littrell, R. H., & Brennemann, T. B. (1990). Utilization of a multispectral radiometer to evaluate fungicide efficacy to control late leaf spot in peanut. *Phytopathology, 80*, 102–108.

Penuelas, J., Baret, F., & Filella, I. (1995). Semiempirical indices to assess carotenoids/chlorophyll a ratio from leaf spectral reflectance. *Photosynthetica, 31*, 221–230.

Pietrzykowski, E., Stone, C., Pinkard, E., & Mohammed, C. (2006). Effects of *Mycosphaerella* leaf disease on the spectral reflectance properties of juvenile *Eucalyptus* globules foliage. *Forest Pathology, 36*, 334–348.

Pinter, P. J., Hatfield, J. L., Schepers, J. S., Barnes, E. M., Moran, M. S., Daugthry, C. S. T., et al. (2003). Remote sensing for crop management. *Photogrammetric Engineering and Remote Sensing, 69*, 647–664.

Richardson, A. D., Duigan, S. P., & Berlyn, G. P. (2001). An evaluation of noninvasive methods to estimate foliar chlorophyll content. *New Phytologist, 153*, 185–194.

Rouse, J. W., Haas, R. H., Schell, J. A., & Deering, D. W. (1974). Monitoring vegetation systems in the Great Plains with ERTS. In *Proceedings of the third earth resources technology satellite-1 symposium* (pp. 301–317). Greenbelt, MD: NASA.

Stafford, J. V. (2000). Implementing precision agriculture in the 21st century. *Journal Agricultural Engineering Research, 76*, 267–275.

Steddom, K., Bredehoeft, M. W., Khan, M., & Rush, C. M. (2005). Comparison of visual and multispectral radiometric disease evaluations of *Cercospora* leaf spot of sugar beet. *Plant Disease, 89*, 153–158.

Steddom, K., Heidel, G., Jones, D., & Rush, C. M. (2003). Remote detection of rhizomania in sugar beets. *Phytopathology, 93*, 720–726.

Thenkabail, P. S., Smith, R. B., & De Pauw, E. (2000). Hyperspectral vegetation indices and their relationship with agricultural crop characteristics. *Remote Sensing of Environment, 71*, 158–182.

Van Kan, J. A. L. (2006). Licensed to kill: The lifestyle of a necrotrophic plant pathogen. *Trends in Plant Science, 11*, 247–253.

West, J. S., Bravo, C., Oberti, R., Lemaire, D., Moshou, D., & McCartney, H. A. (2003). The potential of optical canopy measurement for targeted control of field crop diseases. *Annual Review of Phytopathology, 41*, 593–614.

Wolf, P. F. J., & Verreet, J. A. (2002). The IPM sugar beet model, an integrated pest management system in Germany for the control of fungal leaf diseases in sugar beet. *Plant Diseases, 86*, 336–344.

Zhang, M., Liu, X., & O'Neill, M. (2002). Spectral discrimination of *Phytophthora infestans* infections on tomatoes based on principal component and cluster analyses. *International Journal of Remote Sensing, 23*, 1095–1107.